[CANCER RESEARCH 58, 815–822, February 15, 1998]

herg Encodes a K^+ Current Highly Conserved in Tumors of Different Histogenesis: A Selective Advantage for Cancer Cells?[1]

Laura Bianchi, Barbara Wible, Annarosa Arcangeli, Maurizio Taglialatela, Ferdinando Morra, Pasqualina Castaldo, Olivia Crociani, Barbara Rosati, Laura Faravelli, Massimo Olivotto, and Enzo Wanke[2]

Dipartimento di Fisiologia e Biochimica Generali, Università degli Studi di Milano, Milan, Italy [B. R., L. F., E. W.], Rammelkamp Center for Education and Research, MetroHealth Campus, Case Western Reserve University, Cleveland, Ohio 44109-1998 [L. B., B. W.], Istituto di Patologia Generale, Università degli Studi di Firenze, Florence, Italy [A. A., O. C., M. O.]; and Dipartimento di Neuroscienze, Sezione di Farmacologia, Università degli Studi di Napoli Federico II, Naples, Italy [M. T., F. M., P. C.]

ABSTRACT

The human *ether-a-go-go*-related gene (*herg*) encodes a K^+ current (I_{HERG}) that plays a fundamental role in heart excitability by regulating the action potential repolarization (I_{Kr}); mutations of this gene are responsible for the chromosome 7-linked long QT syndrome (LQT2). In this report, we show that in a variety (n = 17) of tumor cell lines of different species (human and murine) and distinct histogenesis (neuroblastoma, rhabdomyosarcoma, adenocarcinoma, lung microcytoma, pituitary tumors, insulinoma β-cells, and monoblastic leukemia), a novel K^+ inward-rectifier current (I_{IR}), which is biophysically and pharmacologically similar to I_{HERG}, can be recorded with the patch-clamp technique. Northern blot experiments with a human *herg* cDNA probe revealed that both in human and murine clones the very high expression of *herg* transcripts can be quantified in at least three clearly identifiable bands, suggesting an alternative splicing of *HERG* mRNA. Moreover, we cloned a cDNA encoding for I_{IR} from the SH-SY5Y human neuroblastoma. The sequence of this cDNA result was practically identical to that already reported for *herg*, indicating a high conservation of this gene in tumors. Consistently, the expression of this clone in *Xenopus* oocytes showed that the encoded K^+ channel had substantially all of the biophysical and pharmacological properties of the native I_{IR} described for tumor cells. In addition, in the tumor clones studied, I_{IR} governs the resting potential, whereas it could not be detected either by the patch clamp or the Northern blot techniques in cells obtained from primary cell cultures of parental tissues (sensory neurons and myotubes), whose resting potential is controlled by the classical K^+ anomalous rectifier current. This current substitution had a profound impact on the resting potential, which was markedly depolarized in tumors as compared with normal cells. These results suggest that I_{IR} is normally only expressed during the early stages of cell differentiation frozen by neoplastic transformation, playing an important pathophysiological role in the regulatory mechanisms of neoplastic cell survival. In fact, because of its biophysical features, I_{IR}, besides keeping the resting potential within the depolarized values required for unlimited tumor growth, could also appear suitable to afford a selective advantage in an ischemic environment.

INTRODUCTION

It has long been known that cancer cells have remarkably lower resting potentials (V_{REST}) than normal cells from the same tissues, and it has been proposed that this is an essential prerogative for cells destined to unlimited growth (reviewed in Ref. 1). Although an obvious explanation of this feature might be ascribed to type and density of K^+ channels, this topic has been scarcely explored with up-to-date electrophysiological and molecular biology techniques. This scientific gap is particularly amazing in view of the huge knowledge available about K^+ channels and their role in the control of mitogenesis (2, 3). In this field, special attention has been devoted recently to the members of an evolutionarily conserved multigene family of voltage-activated K^+ channels that contribute to the signaling capacity of excitable as well as nonexcitable cells (4). The prototype of one such family is the *Drosophila eag*[3] locus (5), which encodes a K^+ channel protein, the heterologous expression of which in *Xenopus* oocytes produces a voltage-dependent outward K^+ current (6). A number of *eag*-related genes have now been cloned, including: *elk* (*Drosophila*), *m-eag* (mouse), and *herg* (human-*eag*-related gene), which was first isolated from a human hippocampus cDNA library and mapped to chromosome 7 (4).

The first clue that the *herg* gene product may play a role in the regulation of human tissue excitability was provided by Curran *et al.* (7), who found that *herg* mutations were related to an inherited ventricular arrhythmia (LQT2). Heterologous expression of the *herg* product (8) showed that it encodes for a K^+ current (I_{HERG}), the major subunit of I_{Kr} channels, which contribute to the repolarization of cardiac action potential (9). This current is specifically blocked by class III antiarrhythmic drugs, such as sotalol and its analogue E4031, as well as by WAY 123,398 and dofetilide (9, 10).

Evidence for the expression of HERG-like currents in tissues other than those of the heart emerged from the discovery that a current having the biophysical and pharmacological properties of HERG (I_{IR}) was constitutively and highly expressed in neuroblastoma cell lines across various species, from mouse to human, and shared the dependence of the conductance on $[K^+]_o$ and, like the I_{HERG} expressed in *Xenopus* oocytes, was blocked by E4031, WAY-123,398, Cs^+, Ba^{2+}, and La^{3+} (11–14). The voltage-dependent gating of the neuroblastoma I_{IR} was characterized by intrinsic inactivation and activation curves that together make the channel operate within the central region of V_{REST} of neuroblastoma cells (about −40 mV). These gating properties are linked to the mechanisms controlling the cell cycle in such a way that the I_{IR} activation curves vary widely in the cells of unsynchronized populations, whereas the synchronization of cells in the G_1 phase of the cell cycle greatly reduces this variability (12).

We here report that I_{IR} is not only present in a number of different neuroblastoma cell lines but also in tumors of different histogenesis. On the contrary, in normal cells derived from tissues with the same histogenesis as the corresponding tumor cell lines, I_{IR} was undetectable, and V_{REST} was governed by different channels displaying biophysical properties similar to the classical inward rectifier current (IRK). Interestingly, the cloning of a *herg* cDNA from SH-SY5Y human neuroblastoma cells and its expression in *Xenopus* oocytes revealed that *herg* and the corresponding K^+ current are maintained substantially unmodified after the neoplastic transformation, providing a new experimental explanation for the depolarized V_{REST}, which characterizes cancer cells.

Received 6/24/97; accepted 12/16/97.

The costs of publication of this article were defrayed in part by the payment of page charges. This article must therefore be hereby marked *advertisement* in accordance with 18 U.S.C. Section 1734 solely to indicate this fact.

[1] This work was supported by grants from the Associazione Italiana per la Ricerca sul Cancro, Consiglio Nazionale delle Ricerche (finalized project, Applicazioni Cliniche per la Ricerca Oncologica), Ministero dell'Università e della Ricerca Scientifica e Tecnologica, Associazione Italiana contro le Leucemie, and NIH Grant HL36930. L. B. is a PhD student from Dipartimento di Scienze Fisiologiche, Università di Firenze. L. F. and B. R. are PhD students from Dipartimento di Fisiologia e Biochimica Generali, Università di Milano.

[2] To whom requests for reprints should be addressed, at University of Milan, Dipartimento di Fisiologia e Biochimica Generali, Via Celoria 26-20133 Milano, Italy. Phone: 39-2-70644609; Fax: 39-2-70632884; E-mail: enzo.wanke@unimi.it.

[3] The abbreviations used are: *eag*, *ether-a-go-go*; DRG, dorsal root ganglion.

MATERIALS AND METHODS

Cell Culture. The human rhabdomyosarcoma TE671, the mouse neuroblastoma N18TG2 (provided by Prof. G. Augusti-Tocco, Department of Cellular Biology, University of Rome, Rome, Italy), the DRG × neuroblastoma hybrid cell line F11, and the human neuroblastoma SHSY5Y (Prof. G. Tarone, Department of Genetics, Biology and Medical Chemistry, University of Turin, Turin, Italy) were cultured in DMEM containing 4.5 g/l of glucose and 10% FCS (5% for the SHSY5Y). The mouse/rat neuroblastoma-glioma NG108–15 (provided by Prof. Augusti-Tocco) was cultured in DMEM-HAT medium containing 4.5 g/l of glucose and 10% of FCS. The rat pheochromocytoma PC12 and small cell lung cancer cells NCI-N592, GLC8, and H69 (kindly provided by Prof. F Clementi, Department of Pharmacology, University of Milan, Milan, Italy); the pituitary cell lines GH_3, GH_4, and MMQ (kindly provided by Dr. I. S. Login, University of Virginia, School of Medicine, Charlottesville, VA); the human mammary gland adenocarcinoma cells SK-BR-3 and the monoblastic leukemia line FLG29.1 (kindly provided by P. Bernabei, Hematology Unit, Florence, Italy) were all cultured in RPMI 1640 containing 10% horse serum and 5% FCS. The human myotubes were cultured in MEM containing 15% FCS, epidermal growth factor (Life Technologies, Inc.) and insulin (Sigma Chemical Co.). The neonatal rat DRG cells were prepared as described (15). The anterior pituitary cells were dissected from 150-g Wistar rats; dissociated with trypsin (25%), collagenase A (25%), and DNase (2.5%); and incubated for 30 min at 37°C. The resulting suspension was plated onto 35-mm dishes at a density of 3×10^5 cells/ml. The plating medium was DMEM containing 4.5 g/l of glucose and 10% FCS. All of the cells were incubated at 37°C in a humidified atmosphere with 5% CO_2 (10% for SHSY5Y and F11).

Molecular Biology. Total RNA from subconfluent cultures of SH-SY5Y cells was isolated using RNA STAT-60 isolation kit (Tel-Test B, Inc.). Overlapping partial fragments of *herg* cDNA were isolated by means of reverse transcription-PCR using the following oligo pairs (the nucleotide numbers refer to the HERG sequence: accession number U04270): fragment 1, forward primer 5′-GATCGGGCCCCTCAGGATGCCGGTGCGGAGGG-GCCAC-3′ (part of the untranslated region, APAI restriction site, and nucleotides 1 to 21 of the translated region; the starting codon is underlined) and reverse primer 5′-GCCCTTGAGGTCGACAAAGTTGAGGGTG-3′ (nucleotides 1008 to 1035); fragment 2, forward primer in which a *SALI* restriction site was introduced (C instead of G, underlined) 5′-CTCAACTTTGTCGACCT-CAAGGGCGAC-3′ (nucleotides 1013 to 1035) and reverse primer 5′-ACT-CAGGGAAGCCCTTCAGC-3′ (nucleotides 2148 to 2167); and fragment 3, forward primer 5′-TCCAGCGGCTGTACTCGGGC-3′ (nucleotides 1988 to 2007) and reverse primer 5′-GGACCAGAAGTGGTCGGAGAACTC-3′ (nucleotides 2539 to 2562); fragment 4, forward primer 5′-GGCTCCATC-GAGATCGAGATCCTGCGGGGC-3′ (nucleotides 2353 to 2376) and reverse primer 5′-GATCGAATTCCTAACTGCCCGGGTCCGAGCC-3′.

PCR was performed as follows: 35 cycles (95°C, 30 s; 55°C, 30 s; and 72°C, 30 s), followed by a final extension for 10 min at 72°C. The bands of the expected molecular weight were gel purified, subcloned into PCRII (Invitrogen, San Diego, CA), and sequenced. The full-length *herg* cDNA was assembled from the overlapping fragments in a modified pSP64 vector in which two new restriction sites were introduced (*Eco*RV and *Nru*I) 3′ to the poly(A)$^+$ tail. For expression in *Xenopus* oocytes, the construct was linearized using *Nru*I and cRNA prepared with the mMESSAGEmMACHINE *in vitro* transcription kit (Ambion, Austin, TX) with SP6 polymerase. The cRNA was precipitated and resuspended in 0.1 M KCl. The integrity of the cRNA was confirmed, and concentration was estimated on a formaldehyde/agarose gel by comparison with an RNA ladder (Life Technologies, Inc., Gaithersburg, MD).

Northern Blot Analysis. Northern blotting was performed using the NorthernMax kit (Ambion). Five to 20 μg of total RNA from each of the tumor cell lines and rat brain and heart (Ambion) were electrophoresed on a 1% agarose-formaldehyde gel. Ethidium bromide (10 μg/ml) was added to the samples prior to electrophoresis to allow visualization of the total RNA before blotting. The transfer to BrightStar-Plus membranes (Ambion) was carried out using the manufacturer's protocol. The blot was probed with the entire *herg* or a fragment (444 bp) encompassing nucleotides 1691–2135 (accession number U04270), which was obtained by means of PCR amplification from the *herg* plasmid. Both probes were labeled with ^{32}P (DecaPrime kit; Ambion) by means of random priming. Hybridization was overnight at 42°C in the solution provided in the NorthernMax kit at a probe concentration of 2×10^6 cpm/ml. The membrane was washed with the buffers supplied with the kit: twice for 10 min at room temperature in wash buffer I and twice for 20 min at 50°C in wash buffer 2. The transcripts were visualized by autoradiography using Kodak Biomax MS film and an intensifying screen for 16–52 h. Higher stringency conditions (hybridization at 65°C and washing at 65°C) gave similar results.

Patch Clamp Recordings. The currents were recorded at room temperature using an amplifier Axopatch 1-D (Axon Instruments, Inc., Foster City, CA). The whole-cell configuration of the patch-clamp technique was adopted using pipettes, the resistances of which were in the range of 5–10 MΩ. Pipette resistance, cell capacitance, and series resistance errors were carefully compensated for by introducing a compensation of about 80–90% before each voltage clamp protocol run. The cells were perfused with an extracellular solution delivered into the chamber where the cells were plated by means of hypodermic needles inserted into a capillary with a small hole. The standard extracellular solution contained 130 mM NaCl, 2 mM KCl, 2 mM $CaCl_2$, 2 mM $MgCl_2$, 10 mM HEPES-NaOH, and 5 mM glucose 5, pH 7.4. When necessary, the NaCl was replaced by KCl 5 and 40 mM. The standard pipette solution at $[Ca^{2+}]_i = 10^{-7}$ M (pCa 7) contained 120 mM K^+-aspartate, 10 mM NaCl, 2 mM $MgCl_2$, 4 mM $CaCl_2$, 10 mM EGTA-KOH, and 10 mM HEPES-KOH. The junction potential (~−5 mV) was not corrected.

Oocyte Handling and Voltage-Clamp Recordings. The *Xenopus* were anesthetized by immersion in 0.2% tricaine for 15–30 min. The ovarian lobes were digested using 2 mg/ml type 1A collagenase (Sigma Chemical Co.) in a Ca^{2+}-free solution to remove follicle cells. Stage IV and V oocytes were injected with *herg* cRNA (0.1–0.5 μg/μl; 40 nl) and then cultured in Barth's solution (88 mM NaCl 88, 1 mM KCl, 0.4 mM $CaCl_2$, 0.33 mM $Ca(NO_3)_2$, 1 mM $MgSO_4$, 2.4 mM $NaHCO_3$, and 10 mM HEPES, pH 7.4). The oocyte measurements were made 2–5 days after the injection at room temperature using standard two microelectrode voltage-clamp techniques. Glass microelectrodes were filled with 3 M KCl, and their tips were broken to obtain tip resistances of 3–6 MΩ. The oocytes were voltage clamped using a commercially available amplifier (Warner Instrument Corp.). The standard bath solution contained 120 mM NaOH, 2 mM KOH, 1 mM $CaCl_2$, 1 mM $MgCl_2$, 10 mM HEPES, and 122 mM methanesulfonic acid. When necessary, the NaOH was replaced by 5 and 40 mM KOH. During the acquisition and data analysis of both the current- and voltage-clamp recordings, the pClamp (Axon Instruments, Foster City, CA) and Origin (Microcal, Inc., Northampton, MA) software were routinely used on a 486DX2 PC.

RESULTS

Expression of *herg* Transcripts and I_{IR} Currents in Various Neuroblastoma Cell Lines. Using Northern blot analysis and patch clamp recordings, we studied the expression of *herg* transcripts and the corresponding K^+ currents in the following neuroblastoma cell lines: SH-SY5Y and SK-NBE (human); N18T42 and 41A3 (murine); F11 (rat DRG-mouse N18TG2 neuroblastoma hybrid); and NG108–15 (mouse-rat hybrid neuroblastoma-glioma), as shown in Fig. 1*A, bottom.*

The Northern blot of RNA from SH-SY5Y cells showed three bands of 4.4, 2.9, and 2.4 kb, which hybridized to the *herg* probe; the largest band (4.4 kb) was the most intense of the three. The same three bands were also shown by the other human line, SK-NBE (Fig. 1*B, bottom*), although the second band (2.9 kb) was much more prevalent than the others. The existence of multiple transcripts suggests that alternative splicing of *herg* mRNA may occur in human neuroblastomas, with quantitative differences from one cell line to another; the alternative splicing of *herg* mRNA has been suggested for human heart mRNA with two bands of 4.4 and 4.1 kb visible on Northern blots (7). The patch clamp recordings obtained using the protocol shown in Fig. 1*G* revealed no substantial differences in the inward currents of the SH-SY5Y and SK-N-BE cells (Fig. 1, *A* and *B, top*). The mouse and mouse-rat hybrid lines (panels *C–F*) expressed the same I_{IR} profile as the human lines but showed only a single band of 4 kb in the Northern blot. This means that either the fragment of

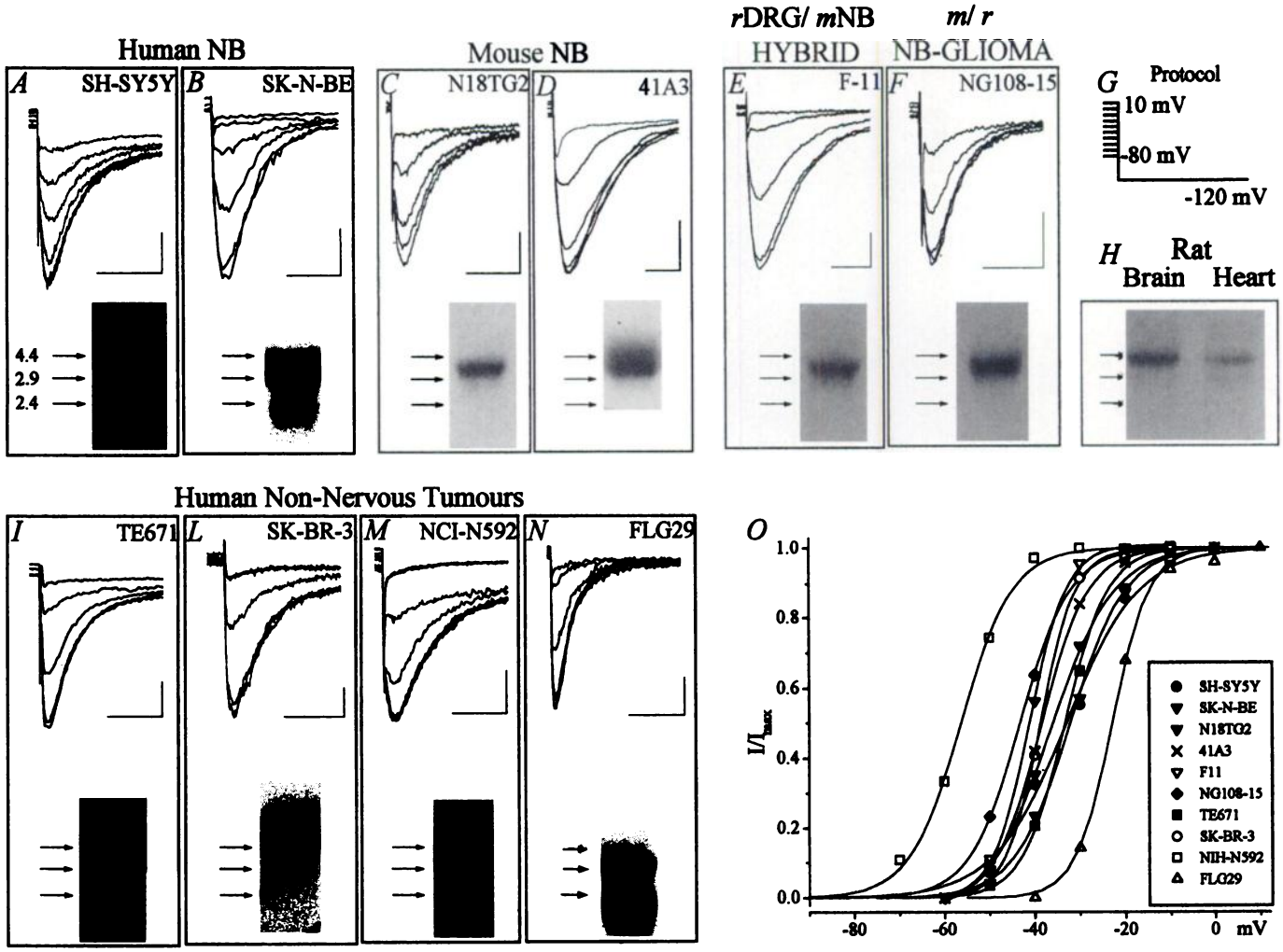

Fig. 1. Expression of *herg* mRNA and the corresponding HERG currents in various tumor cell lines. Each panel shows the I_{IR} currents (*upper*) and Northern blots (*lower*) of each cell type. The currents were elicited in a solution containing 40 mM KCl according to the protocol shown in *G*; the membrane potential was held at various potentials from −80 to −10 for 20 s (preconditioning step) and then stepped up to the test potential (−120 mV) for 200 ms. The Northern blot analyses were performed on total RNA. The blots were hybridized using a ^{32}P-labeled probe encoding the whole sequence or only the region between S3 and S6. The *arrows* on the *left* indicate the molecular weights of the bands observed in SY5Y cells (4.4, 2.9, and 2.4 kb). *H*, Northern blots of rat brain and heart mRNA. In *O*, the experimental points (*symbols*) were obtained from the currents shown in the various *insets* (*A–F* and *I–N*) by plotting their normalized peak amplitude (III_{max}) against the preconditioning potential. The points were then best fitted to Boltzmann equations and gave the following values of $V_{1/2}$ and slope (k; mV) for each of the cell types: SH-SY5Y, −33.1 and 6.7; SK-N-BE, −32 and 6.1; N18TG2, −36.5 and 7.1; 41A3, −38.5 and 5.2; F11, −41 and 4.2; NG108, 15, −43, and 5.1; TE671, −33.3 and 4.74; SK-BR-3, −38.7 and 3.8; NCI-N592, −56.1 and 4.9; FLG29, −23.4 and 4.2. The *scale bars* in *A–F* and *I–N* were 25 ms for time and the following for each cell type (pA): SH-SY5Y, 100; SK-N-BE, 75; N18TG2, 200; 41A3, 150; F11, 200; NG108, 300; TE671, 500; SK-BR-3, 500; NCI-N592, 1000; and FLG29, 100.

human *herg* cDNA used as a probe is not capable of detecting the alternatively spliced transcripts revealed by SH-SY5Y and SK-N-BE RNA or the mouse and/or rat *herg* transcripts are not alternatively spliced. Unlike those of human tissues, Northern blots of rat RNAs from normal tissues known to express *erg*, brain and heart, also show only a single band (Fig. 1*H*). Here the transcript was of about 4.3 kb, which is closer in size to the largest transcript in human tumor cells than to the mRNA detected in mouse/rat neuroblastomas.

Although we did not carry out strictly quantitative comparisons among various cell types, we checked the mRNA load for each sample from the intensity of the 28S and 18S mRNA bands as revealed by ethidium bromide prior to blotting. We considered this procedure the most suitable to have a roughly comparative estimate of *herg* expression in cells of completely different histogenesis, for which it was hard to choose *a priori* a gene expressed at the same level. *herg* expression (Fig. 2*A*) and mRNA loading (Fig. 2*B*) are shown for some of the cell lines reported in Fig. 1 and for normal tissues.

***herg* Expression and I_{IR} in Nonnervous Tumors of Distinct Histogenesis.** The high level of *herg* expression in all of the tested neuroblastoma cell lines prompted us to explore whether *herg* and/or I_{IR} were also detectable in nonnervous tumors of varying histogenesis. As shown in Fig. 1, *I–N*, the tumor cells from human tissues with a completely different histogenesis, such as TE671 rhabdomyosarcoma, SK-BR3 mammary adenocarcinoma, NCI-N592 lung microcytoma, and FLG29 monoblastic leukemia (16), all had transcripts that were detectable using the *herg* probe. The number and relative abundance of *herg* transcripts in all four cell lines was similar to those of the human neuroblastomas except in the case of FLG29, the RNA of which had a unique profile that was characterized by two bands (4.0 and 2.2 kb), of which the smallest was the most prevalent. In all of these nonneuronal tumors, as well as in other clones, including rat pheochromocytoma PC12; small cell lung cancer GLC8 and H69 cells; the GH_3, GH_4, and MMQ pituitary tumors; and RIN and INS-1 pancreatic β-cell tumors (data not shown), I_{IR} was expressed at comparable levels and with the same typical voltage-dependent activation curves as the neuroblastomas. Interestingly, the deactivation

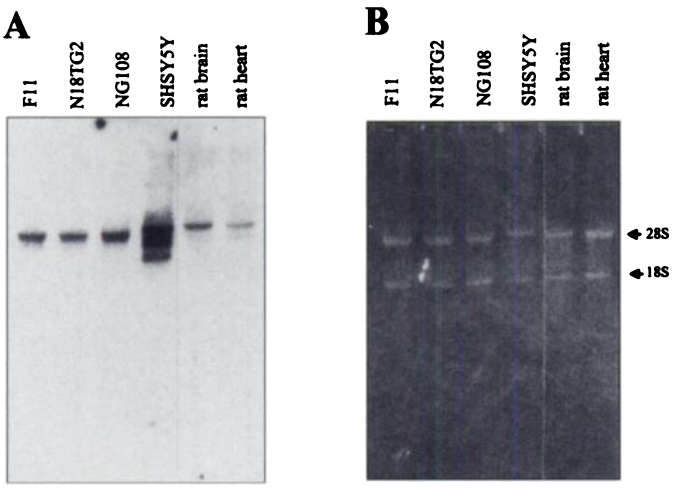

Fig. 2. Northern blot and corresponding mRNA loading for normal and tumor cells. *A*, Northern blot with *herg* probe (see "Materials and Methods") of 5 μg of total mRNA extracted from the tissues indicated in the figure. *B*, the ethidium bromide stained gel prior to blotting. *Arrows*, 28S and 18S RNAs.

time constant was faster in the FLG29 cells (Fig. 1*N*, *top*). Because the smallest transcript in this cell line was the most predominant, the faster deactivation of the resulting I_{IR} is consistent with recent results (17) showing that *herg* transcripts lacking most of the NH_2 terminus have faster deactivation kinetics. Fig. 1*O* shows the currents obtained from tumor cells after they were normalized and plotted against the preconditioning potential to obtain the corresponding voltage-dependent activation curves of I_{IR}. The experimental data were fitted using a Boltzmann equation, which revealed a marked variability in voltage gating among the different cell lines. The most right-shifted curve was for the FLG29 clone, consistent with the faster deactivation referred to above. A similar effect on voltage-dependent gating has been observed in F-11 cells treated with La^{3+} (13). Importantly, the currents shown in Fig. 1 were all pharmacologically identified as HERG currents; all could be blocked by the antiarrhythmics agents E4031 and WAY 123–398, as well as by the inorganic cations Cs^+ and Ba^{2+} in the same way as I_{HERG} and I_{IR} (data not shown; Ref. 13). Our results show that similar I_{IR} currents are expressed at comparable levels in tumors of completely different histogenesis, from neuroblastoma to monoblastic leukemia. These cell lines ostensibly have little in common except the phenotypic characteristics of malignancy, *i.e.*, anaplasia and invasiveness.

Cloning of a *herg* cDNA from SH-SY5Y Human Neuroblastoma Cells. A *herg* cDNA was cloned from SH-SY5Y cells using reverse transcriptase-PCR, for which eight oligonucleotide primers were synthesized on the basis of the *herg* sequence available in the GenBank database (accession number U04270). From the total RNA of SH-SY5Y human neuroblastoma cells, four overlapping cDNA fragments were obtained, sequenced, and assembled into a full-length *herg* coding sequence. The latter resulted to be in some cDNA totally identical to the sequence isolated from human hippocampus by Warmke and Ganetzky (4), whereas in one cDNA clone, we observed a variation of five nucleotides (in boldface and double-underlined letters) as reported in Fig. 3.

This change implies a single amino acid substitution, *i.e.*, an arginine instead of a histidine at position 396 (indicated by the box). This substitution occurs just before the putative S1 segment. It is not yet clear whether these differences are due to mutations introduced during the PCR or represent a true *herg* polymorphism. On the whole, these data suggest that the *herg* in neuroblastoma cells is substantially similar to that originally described in the cDNA of human hippocampus, indicating that this gene is not affected by the transformation process.

Comparison of Native I_{IR} with Currents Expressed by the SH-SY5Y *herg* Clone in *Xenopus* Oocytes. To compare the native I_{IR} currents with those generated by the SH-SY5Y *herg* clone (Fig. 3), we used the heterologous expression in *Xenopus* oocytes.

Fig. 4 shows the inward SH-SY5Y HERG currents recorded in *Xenopus* oocytes compared with the SH-SY5Y I_{IR} current; no comparison of the outward currents is shown because their recording in neuroblastoma cells is complicated by an overlapping delayed rectifying K^+ current that is activated in the same voltage range as HERG. To study the activation properties, we used the protocol described in Fig. 4*C*. The tail currents elicited at −120 mV (Fig. 4*A* for oocytes and Fig. 4*B* for SH-SY5Y cells) were normalized to obtain the activation curves illustrated in Fig. 4*G* (closed and open squares for the oocytes and SH-SY5Y cells, respectively). The inactivation curves (Fig. 4*G*, closed and open triangles for the oocytes and SH-SY5Y cells, respectively) were obtained by plotting the normalized peak chord conductance ($g_{peak} = I_{peak}/[V_M - E_K]$) against the membrane potential V_M (Fig. 4*D* and *E*). The experimental points were fitted to Boltzmann equations, which gave the $V_{1/2}$ and slope values indicated in the figure legend. The shape of the activation curves was identical in the oocytes and SH-SY5Y cells, although the curve was shifted 38 mV to the left in the former. This shift should be not regarded as a peculiarity of the mutated cDNA indicated in Fig. 3 because it was also observed with the unmutated clones (data not shown).

Three possible explanations may account for this shift: (*a*) differences in the internal and/or external surface charge of the plasma membrane that produce changes in the surface potential; (*b*) unique posttranslational modifications of the *herg* gene product in the two cell types; or (*c*) the association of HERG with different subunits in neuroblastoma cells and oocytes.

Activation curves of the *herg* expressed currents reported by Sanguinetti *et al.* (8), Trudeau *et al.* (18), and Schönherr and Heinemann (19) ($V_{1/2}$ = −69 mV *versus* −15, 6, and −19.5, respectively) are shifted to the right as compared with our data obtained from oocyte currents. This discrepancy is explained by the much shorter preconditioning prepulse used in these studies. In fact, we have evidence[4] that shorter prepulses than those shown in Fig. 4*C* (10 s) and a different choice of the V_h (−80 mV *versus* 0 mV in our experiments) led to a rightward shift of the activation curve, because the channels require this amount of time to attain a true steady-state at each voltage. In this light, we consider it a pure chance that the activation curves reported by the cited authors fall close the our SH-SY5Y clone.

Taken together, the properties of the neuroblastoma I_{IR} current were largely reproduced by the currents resulting from the SH-SY5Y *herg* clone.

Neoplastic Transformation Is Accompanied by the Replacement of IRK Currents with I_{IR} Currents: Effects on V_{REST} at Different $[K^+]_o$. As a first insight into the oncological relevance of the recurrent expression of I_{IR} in tumor cells, we conducted a comparative study of the inward K^+ currents in two pairs of histogenetically identical normal and tumor cells, *i.e.*, rDRG *versus* F11 neuroblastoma, and human myotube (HM) *versus* TE671 rhabdomyosarcoma. Interestingly, each of these comparisons revealed that, instead of the I_{IR} recorded in the tumor lines (Fig. 1, *E* and *I*),the normal cells possessed a K^+ current with the biophysical and pharmacological features (Cs^+ sensitive and E-4031 insensitive; data not shown) of the classical inward rectifier IRK (Fig. 5 *A* and *B* and Fig.

[4] B. Rosati, A. Arcangeli, M. Olivotto, and E. Wanke, manuscript in preparation.

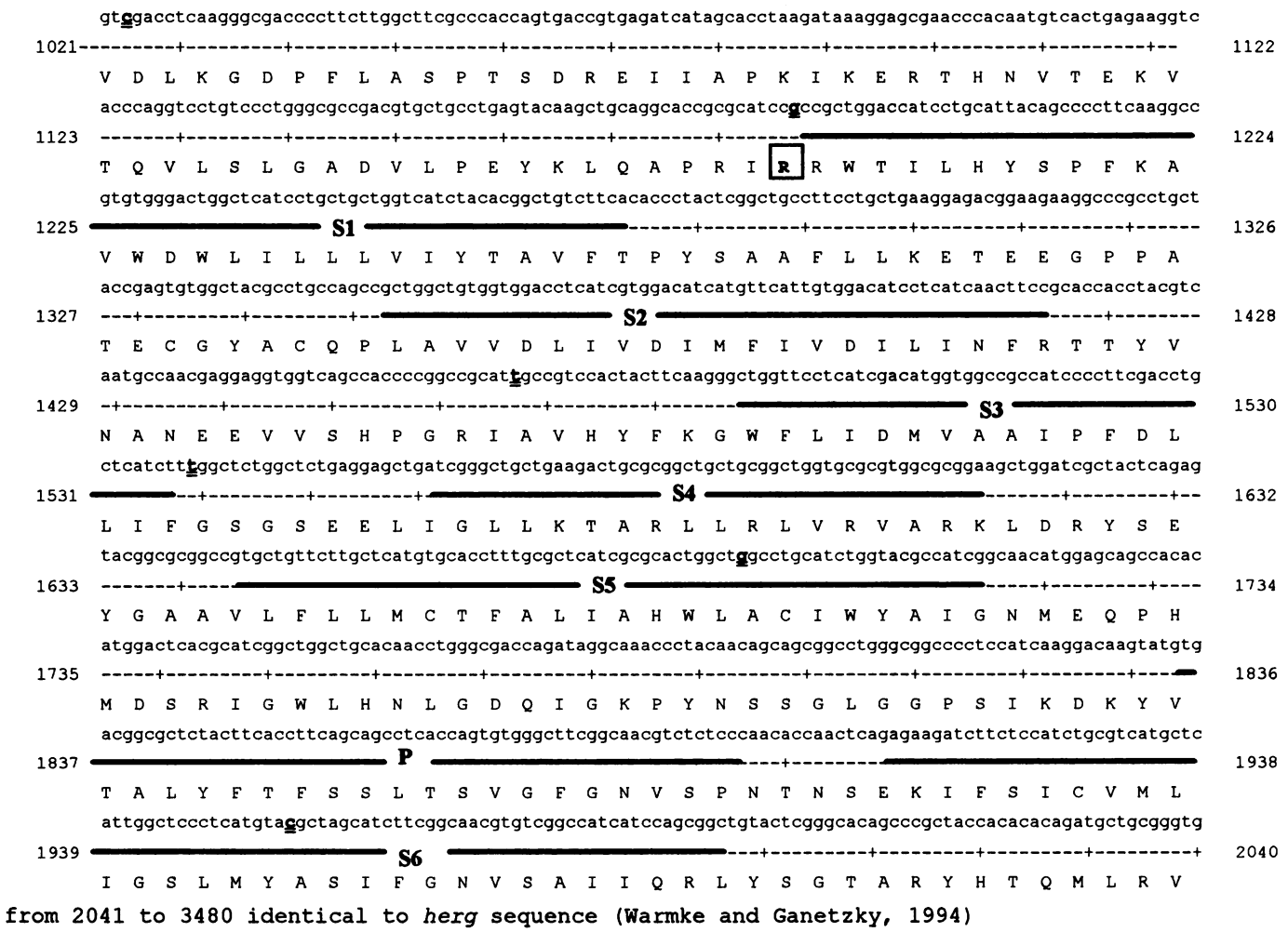

Fig. 3. Nucleotide and amino acid sequence of *herg* from the neuroblastoma clone SH-SY5Y. The differences in nucleotides and amino acids are indicated by *boldface*, *double-underlined letters* and *boxes*, respectively. *Straight lines*, putative transmembrane domains, from S1 to S6.

6*A*). Consistently, *herg* was not found expressed in rDRG and HM cells (Fig. 5*C*).

The impact of this replacement emerged when the cell response to variance of the extracellular K^+ concentration ($[K^+]_o$) was comparatively studied in HM *versus* TE671 rhabdomyosarcoma cells. The *I/V* plot obtained at both physiological and high $[K^+]_o$ (5 mM *versus* 40 mM) of the Cs^+-sensitive IRK steady-state currents recorded from a human myotube showed clear inward rectification with the expected right shift of E_K and the conductance increase at high $[K^+]_o$ (Fig. 6*A*).

A similar experiment performed in a TE671 cell is shown in Fig. 6*B*, which clearly indicates that the steady-state I_{IR} (WAY123.398 sensitive) is active in the V_{REST} region and disappears in the negative region (−55/−70) at both 5 and 40 mM $[K^+]_o$. One consequence of this difference is that V_{REST} can be modulated down to −85 mV by IRK channels in normal cells. In tumor cells without IRK currents, V_{REST} can never be negative to −45 mV because of the deactivation of the HERG channels at these voltages. This is clearly illustrated in Fig. 6*C*, which shows the V_{REST} values of TE671 cells and HM measured as a function of $[K^+]_o$; similar results were also obtained when rDRGs and F11 cells were compared (data not shown).

Thus, neoplastic transformation leads to the regulation of V_{REST} by I_{IR} currents rather than by the IRK-type channels that commonly serve this role in normal differentiated cells, and this change profoundly affects the V_{REST} response to $[K^+]_o$.

Measurements of V_{REST} in Tumors and in Their Normal Counterparts. We have demonstrated that, in neuroblastoma cells, a direct correlation exists between the $V_{1/2}$ of the activation curve of I_{IR} and the value of V_{REST}, so that the more the activation curve was shifted to the right, the more depolarized V_{REST} became (12). Consistent with the observation that most of the tumor cell lines we tested have markedly right-shifted activation curves (Fig. 1*O*), these lines also had rather depolarized V_{REST} values, which were always more positive than −40/−45 mV (Table 1).

This depolarization was emphasized when the V_{REST} values of the tumor cell lines were compared with the normal tissue of corresponding histogenesis [for instance, neuroblastomas clones with rat sensory neurons (rDRG) or TE671 rhabdomyosarcomas with HM].

DISCUSSION

We have shown that *herg* is highly conserved in tumors. The protein encoded by the neuroblastoma clone has the same amino acid sequence as the *herg* cDNA cloned from human hippocampus (4); the only difference in the predicted amino acid sequence is, in one cDNA clone, an arginine replacing histidine at position 396. Whether this replacement is a true polymorphism or a PCR-introduced artifact did not affect the functional properties of the protein because, when expressed in *Xenopus* oocytes, the neuroblastoma *herg* clone pro-

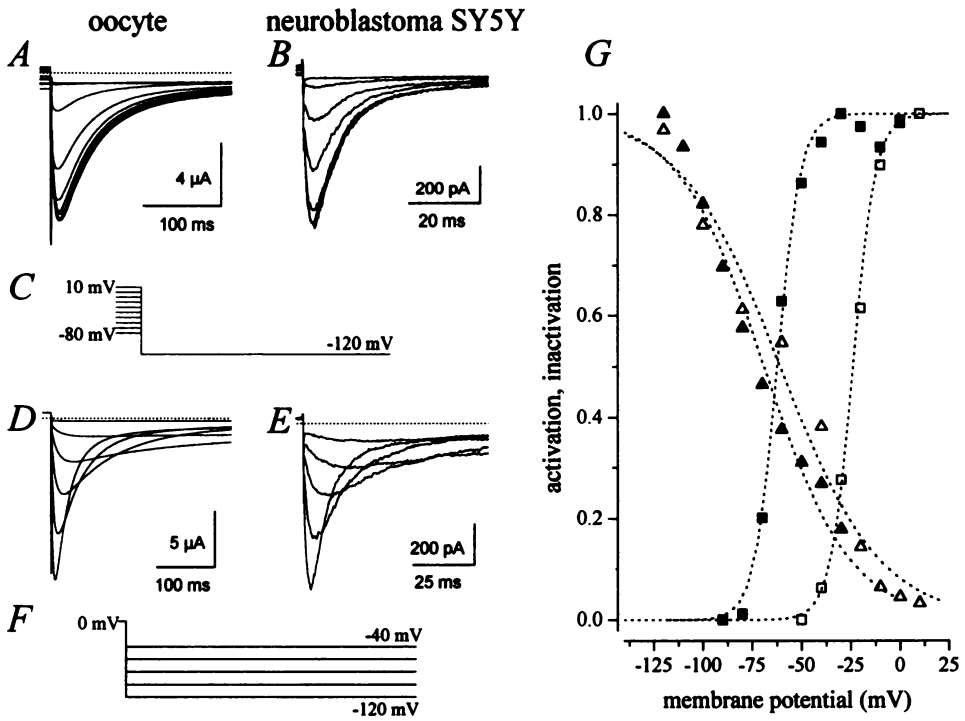

Fig. 4. Comparison of the biophysical properties of currents recorded from oocytes injected with the SH-SY5Y *herg* cRNA and from SH-SY5Y cells. *A* and *B*, currents elicited from oocytes or SH-SY5Y cells according to the protocol shown in *C*. *C*, protocol used for panels *A* and *B*. *D* and *E*, currents elicited according to protocol shown in *F*. *F*, protocol used for panels *D* and *E*. *G*, the normalized activation and inactivation curves of the currents shown in *A–E*. The data points were fitted using a Boltzmann equation, which gave the following values (mV): neuroblastoma SH-SY5Y: inactivation (△) $V_{1/2}$, −61, slope, 25; activation (□) $V_{1/2}$, −24, slope, −5.8; oocyte: inactivation (▲) $V_{1/2}$, −69, slope, 21.7; activation (■) $V_{1/2}$, −62.3, slope, 5.8. $[K^+]_o$ 40 mM.

duced a K^+ current that was identical to that encoded by the hippocampal *herg* clone (8, 18).

The main properties of the I_{IR}, I_{Kr}, and I_{HERG} currents are: (*a*) an activation gate opening upon depolarization and a rapid, hyperpolarization-dependent inactivation that reduces conductances at positive voltages to produce inward rectification; (*b*) sensitivity to class III antiarrhythmic drugs; and (*c*) the $[K^+]_o$ dependence of maximal conductance. These properties make HERG channels unique, because they have the molecular structure of the outward K^+ channel family (six putative transmembrane segments) but show the inward rectification and $[K^+]_o$ dependence that is typical of inward rectifying K^+ channels (which have only two predicted transmembrane segments). The biophysical features of HERG channels readily correlates with cardiac I_{Kr} currents and thus explain their physiological role in the repolarization of the action potential in cardiac myocytes. Moreover, the modulation of I_{Kr} by $[K^+]_o$ may be useful during rapid heart rates or ischemia, when K^+ accumulates within the intracellular clefts (8); under these conditions, the increase in $[K^+]_o$ would enhance the contribution of I_{Kr} to net depolarizing currents.

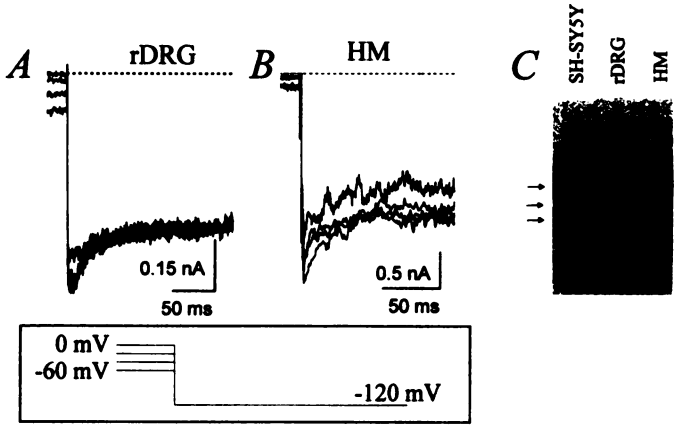

Fig. 5. Sensory neurons and human myotubes do not express *herg*, whereas they display IRK-like currents. *A* and *B*, Cs^+-sensitive currents elicited according to the protocol shown in the *inset* in a rat sensory neuron (*A*, *rDRG*) and a human myotube (*B*, *HM*). These results are typical of the recordings obtained in an additional 9–15 cells for each cell type. Compare this recordings with those shown in Fig. 1, *E* and *I*, respectively. *C*, Northern blot of mRNA obtained with *herg* probe (see "Materials and Methods") for the indicated cell lines. Experimental procedure as shown in Figs. 1 and 2.

The experiments reported in this paper, together with our previous biophysical and pharmacological studies (12, 13), demonstrate that HERG channels are not only operative in heart but also play a role in tumor cells of various lineage (Figs. 1 and 6), because the *herg* transcripts were found to be constitutively expressed in a variety of neuroblastomas as well as in other types of tumors of nonnervous histogenesis.

In tissues representing the normal counterparts of the tested tumors, HERG currents are not detectable by means of the patch-clamp technique, but *herg* have been shown to be present in brain (Fig. 1*H* and Ref. 20). Moreover, in these tissues, HERG channels appear to be substituted by IRK-like currents (Figs. 5 and 6). The presence of IRK-like channels would ensure a more hyperpolarized resting potential in normal cells than in tumor cells; therefore, the occurrence of HERG in tumor cells could certainly contribute to the depolarized V_{REST} that is a feature of cancer cells (1).

In previous reports, we have shown that I_{IR} is functionally linked to neuroblastoma cell integrin receptors, which play a key role in the commitment to differentiate (11, 21). Additional experiments are needed to assess whether this link is a general feature of neoplastic cells that exists as a residual primitive mechanism for signaling cell contact with ECM or other cells (22). This signaling mechanism may consist of the adhesion-mediated activation of a K^+ current with a limited hyperpolarizing power that is capable of influencing voltage-dependent plasma membrane signaling proteins, possibly in localized spots on the cell surface (23, 24). Such a mechanism would be destined to be replaced by more sophisticated signaling devices in mature adherent cells or lost in nonadherent cells. On the contrary, because cancer cells are "frozen" at a more or less primordial stage of differentiation, this mechanism may also be conserved, even in non-adherent cells such as the FLG29 leukemia line.

This view is supported by the transient expression of HERG-like

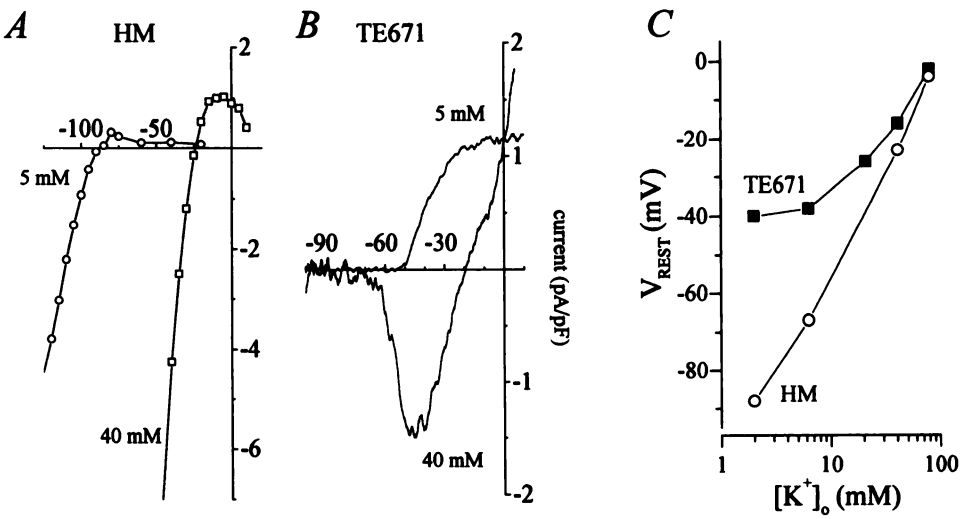

Fig. 6. Currents regulating V_{REST} in tumor and normal cells of the same histogenesis. *A, I/V* plot of the steady-state Cs^+-sensitive current densities recorded in voltage-clamp in a human myotube at two different $[K^+]_o$ of 5 and 40 mM. *B, I/V* plot of the steady-state WAY123–398-sensitive current densities recorded in voltage-clamp in a human rhabdomyosarcoma TE671 cell at two different $[K^+]_o$ of 5 and 40 mM. *C,* V_{REST} measured in two typical TE 671 (□) and HM cells (■) at different $[K^+]_o$.

currents in neuronal and muscle cells at early stages of their development, which are eventually replaced by IRK-like currents (25, 26), and the consequence of this replacement is that the limited hyperpolarizing power of HERG channels is substituted by the limitless power of channels, such as IRK, in fully differentiated cells. The IRK currents can in fact maintain the strongly hyperpolarized V_{REST} that is necessary to fix the voltage in a stable long-lasting state, ready to trigger the action potential. On the other hand, the limited hyperpolarization power of HERG channels may be more appropriate for immature cells, which are unable to generate action potentials and require greater flexibility. In other words, HERG channels may be more suitable for maintaining immature, unstable connections of neurons in nascent synapses, rather than for the stable organized connections that sustain adult brain functions (27). We provided evidence that I_{HERG} reduces the long-lasting firing that neuroblastoma cells acquire upon retinoic acid-mediated differentiation (14); this agrees with the hypothesis that I_{HERG} maintains immature neuronal cells in a state of minimal excitability compatible with a certain proliferative capacity, whereas its replacement by IRK favors a more physiological V_{REST} that characterizes neuronal maturation but also implies the definitive cell exit from the mitotic cycle.

Although the above considerations might account for the persistence of I_{IR} in neuroblastomas, they do not explain the advantage of I_{IR} maintenance in nonnervous tumors. However, the government of V_{REST} by I_{IR} clamps this potential at rather depolarized values (Table 1), which are within the limits required for a continuos cell recruitment into the mitotic cycle. Moreover, the dependence of the conductance of HERG channels on $[K^+]_o$ may confer a selective advantage to tumor cells of any origin. In fact, tumor cells *in vivo* are exposed to severe ischemia, and hence, to K^+ accumulation in the extracellular fluid (28), as a result of imperfect angiogenesis and uncontrolled cell proliferation (29–32). Under these conditions and adopting the reasoning of Sanguinetti *et al.* (8), a $[K^+]_o$-driven mechanism of cell hyperpolarization may be crucial to cell survival. When the ATP shortage produced by ischemia leads to Na^+/K^+ pump failure, K^+ loss from the cell may be counterbalanced by the hyperpolarization elicited by the increase in HERG conductance.

To conclude, the high level of HERG expression in tumor cells may represent a selective advantage for transformed clones, a speculation that deserves an experimental demonstration.

Table 1 *Current-clamp measurements (mean ± SE) of V_{REST} measured at physiological $[K^+]_o$ (5 mM)*

	V_{REST} (mV)	*n*
Cancer cells		
SH-SY5Y	−28.5 ± 1.8	20
NG108-15	−38 ± 5	8
N18TG2	−40.8 ± 5	8
PC12	−34 ± 5.3	5
41A3	−41.8 ± 0.9	47
F11	−46 ± 3.4	5
TE671	−36 ± 6	6
Normal cells		
Human myotubes (HM)	−62 ± 6	10
Sensory neurons (rDRG)	−58 ± 1.4	25

ACKNOWLEDGMENTS

We are indebted to Arthur M. Brown, A. Ferroni, and A. Fonnesu for valuable support. We also thank Dr. E. Mancinelli for the human myotubes, S. Dubel for molecular biology support, W. Q. Dong and C-D. Zuo for oocyte handling and injection, and G. Mostacciuolo for technical improvements.

REFERENCES

1. Binggeli, R., and Weinstein, R. C. Membrane potentials and sodium channels: hypotheses for growth regulation and cancer formation based on changes in sodium channels and gap junctions. J. Theor. Biol., *123:* 377–401, 1986.
2. Jan, L. Y., and Jan, Y. N. Cloned potassium channels from eukaryotes and prokaryotes. Annu. Rev. Neurosci., *20:* 91–123, 1997.
3. Dubois, J. M., and Rouzaire-Dubois, B. Role of potassium channels in mitogenesis. Prog. Biophys. Mol. Biol., *59:* 1–21, 1993.
4. Warmke, J. W., and Ganetzky, B. A family of potassium channel genes related to *eag* in *Drosophila* and mammals. Proc. Natl. Acad. Sci. USA, *91:* 3438–3442, 1994.
5. Ganetzky, B., and Wu, C. F. Neurogenetic analysis of potassium currents in Drosophila: synergistic effects on neuromuscular transmission in double mutants. J. Neurogenet., *1:* 7–28, 1983.
6. Ludwig, J., Terlau, H., Wunder, F., Brueggeman, A., Pardo, L. A., Marquardt, A., Stuehmer, W., and Pongs, O. Functional expression of a rat homologue of the voltage gated *ether à gogo* potassium channels reveals differences in selectivity and activation kinetics between the *Drosophila* channel and its mammalian counterpart. EMBO J., *13:* 4451–4458, 1994.
7. Curran, M. E., Splawski, I., Timothy, K. W., Vincent, G. M., Green, E. D., and Keating, M. K. A molecular basis for cardiac arrhythmia: HERG mutations cause long QT syndrome. Cell, *80:* 95–804, 1995.
8. Sanguinetti, M. C., Jiang, C., Curran, M. E., and Keating, M. T. A mechanistic link between an inherited and acquired cardiac arrhythmia: HERG encodes the Ikr potassium channel. Cell, *81:* 299–307, 1995.
9. Sanguinetti, M. C., and Jurkiewicz, N. K. Two components of cardiac delayed rectifier K^+ current. J. Gen. Physiol., *96:* 195–215, 1990.
10. Spinelli, W., Moubarak, I. F., Parson, R. W., and Colatsky, T. J. Cellular electrophysiology of WAY 123,398, a new class III antiarrhythmic agent: specificity and frequency-independence of Ik block in cat ventricular myocytes. Cardiovasc. Pharmacol., *27:* 1580–1589, 1993.
11. Arcangeli, A., Becchetti, A., Mannini, A., Mugnai, G., De Filippi, P., Tarone, G., Del Bene, M. R., Barletta, E., Wanke, E., and Olivotto, M. Integrin-mediated neurite outgrowth in neuroblastoma cells depends on the activation of potassium channels. J. Cell Biol., *122:* 1131–1143, 1993.

12. Arcangeli, A., Bianchi, L., Becchetti, A., Faravelli, L., Coronnello, M., Mini, E., Olivotto, M., and Wanke, E. A novel inward-rectifying K^+ current with a cell cycle-dependence governs the resting potential of neuroblastoma cells. J. Physiol., *489:* 455–471, 1995.
13. Faravelli, L., Arcangeli, A., Olivotto, M., and Wanke, E. A HERG-like channel in rat F-11 DRG cell line: pharmacological identification and biophysical characterisation. J. Physiol., *496:* 13–23, 1996.
14. Chiesa, N., Rosati, B., Arcangeli, A., Olivotto, M., and Wanke, E. A novel role for HERG K^+ channels: spike frequency adaptation. J. Physiol., *501:* 313–318, 1997.
15. Wanke, E., Becchetti, A., Biella, G., Del Bo, R., and Ferroni, A. A quantitative description of low- and high-threshold Ca^{2+} spikes in rat sensory neurons: a perforated-patch study. Eur. J. Neurosci., *4:* 723–732, 1992.
16. Gattei, V., Bernabei, P. A., Pinto, A., Bezzini, A., Ringressi, A., Formigli, A., Attadia, V., and Brandi, M. L. Phorbol ester induced osteoclast-like differentiation of a novel human leukaemia cell line (FLG29.1). J. Cell Biol., *116:* 437–447, 1992.
17. Trudeau, M. C., London, B., Beyer, A. K., Newton, K. P., and Robertson, G. A. Expression of HERG homologs cloned from the mouse. Biophys. J., *72:* A224, 1997.
18. Trudeau, M. C., Warmke, J. W., Ganetzky, B., and Robertson, G. A. HERG, a human inward rectifier in the voltage-gated potassium channel family. Science (Washington DC), *269:* 92–95, 1995.
19. Schönherr, R., and Heinemann, S. H. Molecular determinants for activation and inactivation of a human inward rectifier potassium channel. J. Physiol., *493:* 653–642, 1996.
20. Wymore, R. S., Gintant, G. A., Wymore, R. T., Dixon, J. E., Mckinnon, D., and Cohen, I. S. Tissue and species distribution of mRNA for the IKr-like K^+ channel ERG. Circ. Res., *80:* 261–268, 1997.
21. Bianchi, L., Arcangeli, A., Bartolini, P., Mugnai, G., Wanke, E., and Olivotto, M. An inward rectifier K^+ current modulates in neuroblastoma cells the tyrosine phosphorylation of the $pp125^{FAK}$ and associated protein: role in neuritogenesis. Biochem. Biophys. Res. Commun., *210:* 823–829, 1995.
22. Hynes, R. O. Integrins: versatility, modulation and signalling in cell adhesion. Cell, *69:* 11–25, 1992.
23. Olivotto, M., Arcangeli, A., Carlà, M., and Wanke, E. Electric fields at the plasma membrane level: a reappraisal of a neglected key to decipher the mechanisms of cell signalling. BioEssays, *18:* 495–504, 1996.
24. Arcangeli, A., Faravelli, L., Bianchi, L., Rosati, B., Gritti, A., Vescovi, A., Wanke, E., and Olivotto, M. Soluble or bound laminin elicit in human neuroblastoma cells short- or long-term potentiation of a K^+ inwardly rectifying current: relevance to neuritogenesis. Cell Adhes. Commun., *4:* 369–385, 1996.
25. Wanke, E., Arcangeli, A., Olivotto, M., Faravelli, L., and Bonecchi, R. A HERG-like K^+ current in proliferating myoblasts before fusion. Soc. Neurosci. Abstr., *22:* 571.2, 1996.
26. Arcangeli, A., Rosati, B., Cherubini, A., Crociani, O., Fontana, L., Ziller, C., Wanke, E., and Olivotto, M. HERG- and IRK-like inward rectifier currents are sequentially expressed during neuronal development of neural crest cells and derivatives. Eur. J. Neurosci., *9:* in press, 1997.
27. Katz, L. C., and Shatz, C. J. Synaptic activity and the construction of cortical circuits. Science (Washington DC), *274:* 1133–1138, 1996.
28. Hansen, A. K. Effect of anoxia on ion distribution in the brain. Physiol. Rev., *65:* 101–148, 1987.
29. Vaupel, P., Kallinowski, F., and Okunieff, P. Blood flow, oxygen, nutrient supply, and metabolic microenvironment of human tumors: a review. Cancer Res., *49:* 6449–6465, 1989.
30. Coleman, C. N. Hypoxia in tumors: a paradigm for the approach to biochemical and physiological heterogeneity. J. Natl. Cancer Inst., *80:* 310–317, 1988.
31. Dewhirst, M. W, Secomb, T. W., Ong, E. T., Hsu, R., and Gross, J. F. Determination of local oxygen consumption rates in tumors. Cancer Res., *54:* 3333–3336, 1994.
32. Lyng, H., Sundfor, K., Tropé, C., and Rofstad, E. K. Oxygen tension and vascular density in human cervix carcinoma. Br. J. Cancer, *74:* 1559–1563, 1996.